Genomic Characterization of Cholangiocarcinoma in Primary Sclerosing Cholangitis Reveals Therapeutic Opportunities

Benjamin Goeppert,[1*] Trine Folseraas,[2-6*] Stephanie Roessler,[1*] Matthias Kloor,[7] Anna-Lena Volckmar,[1] Volker Endris,[1] Ivo Buchhalter,[1,8] Albrecht Stenzinger,[1] Krzysztof Grzyb,[9] Marit M. Grimsrud,[2-4] Barbara Gornicka,[10] Erik von Seth,[11] Gary M. Reynolds,[12] Andre Franke,[13] Daniel N. Gotthardt,[14] Arianeb Mehrabi,[15] Angela Cheung,[16] Joanne Verheij,[17] Johanna Arola,[18] Heikki Mäkisalo,[19] Tor J. Eide,[9] Sören Weidemann,[20] John C. Cheville,[21] Giuseppe Mazza,[22] Gideon M. Hirschfield,[12,23] Cyriel Y. Ponsioen,[24] Annika Bergquist,[11] Piotr Milkiewicz,[25,26] Konstantinos N. Lazaridis,[16] Christoph Schramm,[27,28] Michael P. Manns,[29] Martti Färkkilä,[30] Arndt Vogel,[29] International PSC Study Group,[31] Kirsten M. Boberg,[2-6] Peter Schirmacher,[1**] and Tom H. Karlsen[2-6**]

BACKGROUND AND AIMS: Lifetime risk of biliary tract cancer (BTC) in primary sclerosing cholangitis (PSC) may exceed 20%, and BTC is currently the leading cause of death in patients with PSC. To open new avenues for management, we aimed to delineate clinically relevant genomic and pathological features of a large panel of PSC-associated BTC (PSC-BTC).

APPROACH AND RESULTS: We analyzed formalin-fixed, paraffin-embedded tumor tissue from 186 patients with PSC-BTC from 11 centers in eight countries with all anatomical locations included. We performed tumor DNA sequencing at 42 clinically relevant genetic loci to detect mutations, translocations, and copy number variations, along with histomorphological and immunohistochemical characterization. Regardless of the anatomical localization, PSC-BTC exhibited a uniform molecular and histological characteristic similar to extrahepatic cholangiocarcinoma. We detected a high frequency of genomic alterations typical of extrahepatic cholangiocarcinoma, such as *TP53* (35.5%), *KRAS* (28.0%), *CDKN2A* (14.5%), and *SMAD4* (11.3%), as well as potentially druggable mutations (e.g., *HER2/ERBB2*). We found a high frequency of nontypical/nonductal histomorphological subtypes (55.2%) and of the usually rare BTC precursor lesion, intraductal papillary neoplasia (18.3%).

CONCLUSIONS: Genomic alterations in PSC-BTC include a significant number of putative actionable therapeutic targets. Notably, PSC-BTC shows a distinct extrahepatic morpho-molecular phenotype, independent of the anatomical location of the tumor. These findings advance our understanding of PSC-associated cholangiocarcinogenesis and provide strong incentives for clinical trials to test genome-based personalized treatment strategies in PSC-BTC. (HEPATOLOGY 2020;72:1253-1266).

Primary sclerosing cholangitis (PSC) is a chronic cholestatic liver disease, often associated with inflammatory bowel disease.[1] In the absence of

any effective medical treatment, progressive bile duct injury and cholestasis lead to end-stage liver disease in most patients. In addition, patients with PSC experience a greatly increased risk of neoplasia arising from the biliary epithelium, including cholangiocarcinoma (CCA) and gallbladder carcinoma (GBC). Malignancy reduces overall patient survival significantly and currently serves as the most frequent cause of PSC-related death.[2] The reported cumulative risk of BTC development in PSC ranges from 6%-22% for CCA and 1%-4% for GBC.[1,3,4] Patients with PSC are young, and the high risk of an often incurable cancer poses an important unmet clinical need. The pathophysiological basis of the high risk of BTC in PSC is not clear, but chronic inflammation in the context of the biliary microenvironment is likely to play a key role.

ARTICLE INFORMATION:

From the [1]Department of General Pathology, Institute of Pathology, University Hospital Heidelberg, Heidelberg, Germany; [2]Norwegian PSC Research Center Department of Transplantation Medicine, Division of Surgery, Inflammatory Medicine and Transplantation, Oslo University Hospital Rikshospitalet, Oslo, Norway; [3]Institute of Clinical Medicine, Faculty of Medicine, University of Oslo, Oslo, Norway; [4]Research Institute of Internal Medicine, Division of Surgery, Inflammatory Medicine and Transplantation, Oslo University Hospital Rikshospitalet, Oslo, Norway; [5]K.G. Jebsen Inflammation Research Center, Institute of Clinical Medicine, Faculty of Medicine, University of Oslo, Oslo, Norway; [6]Section for Gastroenterology, Department of Transplantation Medicine, Division of Surgery, Inflammatory Medicine and Transplantation, Oslo University Hospital Rikshospitalet, Oslo, Norway; [7]Department of Applied Tumor Biology, Institute of Pathology, University of Heidelberg, Heidelberg, Germany; [8]Institute of Pathology, Omics IT and Data Management Core Facility, German Cancer Research Center (DKFZ), Heidelberg, Germany; [9]Department of Pathology, Oslo University Hospital, Oslo, Norway; [10]Department of Pathology, Medical University of Warsaw, Warsaw, Poland; [11]Department of Gastroenterology and Hepatology, Karolinska Institutet, Karolinska University Hospital, Stockholm, Sweden; [12]Center for Liver Research, NIHR Birmingham Liver Biomedical Research Unit, University of Birmingham, Birmingham, United Kingdom; [13]Institute of Clinical Molecular Biology, Christian-Albrechts University, Kiel, Germany; [14]Department of Internal Medicine IV, University Hospital Heidelberg, Heidelberg, Germany; [15]Department of General, Visceral and Transplantation Surgery, University of Heidelberg, Heidelberg, Germany; [16]Division of Gastroenterology and Hepatology, Mayo Clinic, Rochester, MN; [17]Department of Pathology, Academic Medical Center, Amsterdam, the Netherlands; [18]Department of Pathology, Haartman Institute and Huslab, Helsinki University Hospital, Helsinki, Finland; [19]Department of Transplantation and Liver Surgery, Helsinki University Hospital, Helsinki, Finland; [20]Institute of Pathology, University Medical Center Hamburg-Eppendorf, Hamburg, Germany; [21]Department of Laboratory Medicine and Pathology, Mayo Clinic, Rochester, MN; [22]Division of Medicine, Institute for Liver and Digestive Health Royal Free Hospital, University College London, London, United Kingdom; [23]University Hospital Birmingham, NHS Foundation Trust, Birmingham, United Kingdom; [24]Department of Gastroenterology and Hepatology, Academic Medical Center, Amsterdam, the Netherlands; [25]Liver and Internal Medicine Unit, Medical University of Warsaw, Warsaw, Poland; [26]Translational Medicine Group, Pomeranian Medical University, Szczecin, Poland; [27]Department of Medicine, University Medical Center Hamburg-Eppendorf, Hamburg, Germany; [28]Martin Zeitz Center for Rare Diseases, University Medical Center Hamburg-Eppendorf, Hamburg, Germany; [29]Department of Gastroenterology, Hepatology and Endocrinology, Hannover Medical School, Hannover, Germany; [30]Department of Gastroenterology & Hepatology, Helsinki University Hospital, Helsinki, Finland; [31]www.ipscsg.org.

ADDRESS CORRESPONDENCE AND REPRINT REQUESTS TO:

Tom H. Karlsen, Ph.D.
Department of Transplantation Medicine, Division of Surgery
Inflammatory Medicine and Transplantation, Oslo University
Hospital Rikshospitalet

Postboks 4950 Nydalen
N-0424 Oslo, Norway
E-mail: t.h.karlsen@medisin.uio.no
Tel.: +47-23073616

In the United States and Europe, CCA is generally considered relatively rare (less than 6 per 100,000 population), with PSC as a predominant risk factor.[5] CCA is more frequent in Southeast Asia (up to 113 per 100,000 person-years), primarily due to endemic fluke infections with *Opisthorchis viverrini* or *Clonorchis sinensis*.[6] The main subtypes of CCA are represented by extrahepatic CCA, including perihilar CCA (pCCA or Klatskin tumors) and distal extrahepatic CCA (dCCA), and intrahepatic CCA (iCCA). The spectrum of subtypes of CCA in PSC have not been precisely defined, but tumors are frequently located in the perihilar and distal extrahepatic regions. Histologically, CCA and GBC from other etiologies consist of ductal/glandular/tubular/acinar (i.e., not otherwise specified [NOS]) adenocarcinomas in about 90% of cases, whereas the histologic patterns of PSC-BTC have not yet been evaluated in comprehensive cohorts. Although there are data that suggest there are effective measures for surveillance of cholangiocarcinoma in PSC, it is notoriously difficult to differentiate benign from malignant biliary strictures, leading to late diagnosis in most cases.[7] Surgery either by resection or liver transplantation represents the only curative intent treatment for PSC-CCA. Only one-third of the patients are candidates for radical surgery at the time of CCA diagnosis, and the local recurrence rate after surgery is above 60%.[8] Liver transplantation following neoadjuvant radiotherapy with chemosensitization may provide improved survival for highly selected patients with early-stage, unresectable perihilar CCA.[9] The benefit of current palliative systemic chemotherapy regimens is limited, with median overall survival less than 12 months using first-line treatment with gemcitabine and cisplatin.[10]

As an established branch of personalized medicine, profiling of somatic mutations in tumor DNA has identified clinically relevant genomic alterations in key pathways of prognostic and therapeutic relevance.[11] In BTC derived from other etiologies than PSC, several molecular genetic alterations have been identified across multiple tumor-suppressor genes and oncogenes, such as *KRAS* (Kirsten rat sarcoma viral oncogene homolog), *TP53* (tumor protein 53), *SMAD4* (mothers against decapentaplegic homolog 4), *CDKN2A* (cyclin-dependent kinase inhibitor 2A), *ERBB1/2* (erythroblastic leukemia viral oncogene homolog 1/2), *FGFR* (fibroblast growth factor receptor), and *IDH1/2* (isocitrate dehydrogenase 1/2).[11-14] Previous efforts have revealed that genomic alterations in BTC differ according to the anatomical subtypes of BTC and causative etiology, guiding the transformation of findings from different anatomical and etiological subtypes into diagnostic and treatment algorithms.[11,15] As such, molecular profiling of different BTC subtypes highlights different clusters of genomic alterations that converge into functional categories that may enable future precision oncology approaches.[14]

The fraction of PSC patients in exome-sequencing studies of BTC has been low (less than 2% known cases with underlying PSC).[11,14] Given the prospects for diagnostic and therapeutic improvements for patients with PSC, we herein aimed to integrate findings from these studies with generic cancer-gene panels to perform a focused assessment of clinically relevant mutations in PSC-associated BTC using targeted resequencing. We hypothesized that an enhanced understanding of the molecular carcinogenesis would delineate molecular driver lesions of relevance and potentially identify druggable targets.

Materials and Methods

PATIENT SAMPLES AND CLINICOPATHOLOGICAL DATA

We used archived, formalin-fixed, paraffin-embedded (FFPE) specimens obtained from explanted livers, partial liver resections, cholecystectomies, or biopsies performed between 1996 and 2016 for the purpose of diagnosis or treatment of PSC-BTC. In total, we collected 224 PSC-BTC samples from 11 centers in Europe and the United States. After initial analysis, 38 samples were excluded based on the histomorphological criteria (mostly insufficient tumor material), tumor cellularity less than 10%, or low DNA content or quality (total dropout rate of 17%). The final panel submitted to further mutational profiling, consisting of 186 PSC-BTC tissue specimens. Clinical follow-up data were available for 160 patients.

Diagnosis of PSC was based on standard clinical, biochemical, cholangiographic, and histological criteria.[8] Detailed clinical data and histopathological information were available for 174 patients (Tables 1 and 2 and Supporting Table S1). Two board-certified pathologists (B.G. and P.S.) validated the histopathological diagnosis of CCA and GBC. Staging of the tumors was performed according to the American Joint Committee on Cancer (AJCC) classification, 8th edition.

Number (Percent)	Invasive (n = 174)	HGD (n = 12)
Tumor subtype		
iCCA	60 (32.3)	—
pCCA	64 (34.4)	6 (3.2)
dCCA	18 (9.7)	—
xCCA	4 (2.2)	1 (0.5)
GBC	28 (15.1)	5 (2.7)
Sampling procedure*		
Biopsy	36 (19.4)	1 (0.5)
Resection	96 (51.6)	8 (4.3)
Liver explant	42 (22.6)	3 (1.6)

Note: HGD = high-grade noninvasive biliary neoplasia (i.e., IPNB or BilIN-3).
*Sampling procedure of the analyzed samples according to an assessment of the histological material and available clinicopathological data.
Abbreviations: xCCA, cholangiocarcinoma of unknown anatomical subtype.

ETHICAL APPROVAL

Written informed consent was obtained from all study subjects at each center if possible. For long-time archived samples, where this was not possible, an exemption from informed consent was obtained by the local ethical committee to allow the use of the samples. Study protocols were approved by the ethics committees of all recruiting centers as well as the Regional Committees for Medical and Health Research Ethics of South East Norway (6.2008.1723) and the ethical board of the University Hospital Heidelberg, Germany (206/05).

PANEL SEQUENCING

For DNA and RNA extraction and processing, see Supporting Information. Massive parallel sequencing was performed using three panels: (1) a custom PSC-BTC panel that consisted of 284 primer pairs (amplicons) covering 165 exons of 40 genes frequently mutated in hepato-pancreatobiliary cancers (2), a custom panel covering 27 hepatobiliary cancer–associated gene translocations, and (3) the commercial Oncomine BRCA (breast cancer antigen) panel covering all exons of *BRCA1* (113 amplicons) and *BRCA2* (152 amplicons) (Thermo Fisher Scientific, Waltham, MA) (see Supporting Table S2). All variants were inspected manually using the IGV browser, and the limit of detection

was set at 5% to avoid false-positive results due to C > T transitions (deamination artifacts introduced by formalin fixation).

IMMUNOHISTOCHEMISTRY, CHROMOGEN *IN SITU* HYBRIDIZATION, AND MOLECULAR MICROSATELLITE INSTABILITY ANALYSIS

Tissue microarrays (TMAs) were fabricated for all 95 cases of which sufficient tissue block material was available (Supporting Table S3). For immunohistochemical (IHC) staining and chromogen *in situ* hybridization (CISH), 3-μm sections of the TMA were used.

Technical details of the IHC and CISH analyses are provided in the Supporting Information and in Supporting Tables S3 and S5. For details on the molecular microsatellite instability (MSI) analysis, see the Supporting Information.

STATISTICAL ANALYSIS

The extensive tissue panel with samples from tumors originating from all anatomical subsites allowed for subgroup assessments, including analyses of frequencies of mutations and interrelationship of mutations among the anatomical subtypes. Graphical representations of mutational frequencies in the total BTC panel and in the anatomical BTC subtypes by oncoplot, circos plots, and PCA were created by the publicly available R-packages ComplexHeatmap, circlize, and factoextra (Figs. 1 and 2 and Supporting Fig. S4). Due to limitations in visualizing multidimensional data, only pair-wise co-occurrences are represented in the circos plots. Frequencies shown by the oncoplots are on a sample per-gene basis and do not take into account that some genes may contain more than one mutation in the same tumor sample.

The publicly available data of Wardell et al., J Hepatology 2018 were analyzed for the 12 genes with highest frequencies of alterations in our panel (*TP53, KRAS, CDKN2A, SMAD4, PIK3CA* [phosphoinositide-3-kinase, catalytic, alpha polypeptide], *CDKN2B, ERBB2, ROBO1* [roundabout homolog 1], *KDM6A* [lysine demethylase 6A], *FBXW7* [F-box and WD repeat domain containing 7], *GNAS* [guanine nucleotide binding protein (G protein), alpha

TABLE 2. Clinical and Histopathological Data of the PSC-BTC Panel (n = 174)

	Number (Percent)
Patients with PSC*	174 (100.0)
Mean age at BTC diagnosis	48.1 years
Overall survival[†]	
2-year survival (%)	47.0
5-year survival (%)	21.6
Sex	
Male	128 (73.6)
Female	46 (26.4)
Operation procedure[‡]	
Biospy	34 (19.5)
Resection	84 (48.3)
Liver transplantation	56 (32.2)
Subtype	
iCCA	60 (34.5)
pCCA	64 (36.8)
dCCA	18 (10.3)
xCCA	4 (2.3)
GBC	28 (16.1)
Histology	
NOS[‖]	74 (42.5)
Papillary	23 (13.2)
Mucinous	41 (23.6)
Solid	19 (10.9)
Diffuse	7 (4.0)
Intestinal	3 (1.7)
Adenosquamous	3 (1.7)
NA	4 (2.3)
AJCC[§]	
AJCC 0	3 (1.7)
AJCC 1	9 (5.1)
AJCC 2	22 (12.5)
AJCC 3	45 (25.6)
AJCC 4	38 (21.6)
NA	57 (32.4)
pT	
T1	18 (10.2)
T2	54 (30.7)
T3	32 (18.2)
T4	17 (9.7)
NA	53 (30.1)
pN	
N0	46 (26.1)
N1	67 (38.1)
NA	61 (34.7)
M	
M0	93 (52.8)
M1	38 (21.6)
NA	43 (24.4)

TABLE 2. *Continued*

	Number (Percent)
G	
G1	3 (1.7)
G2	131 (74.4)
G3	36 (20.5)
NA	4 (2.3)
R	
R0	18 (10.2)
R1	11 (6.3)
R2	5 (2.8)
NA	140 (79.5)
L/V	
L/V0	14 (8.0)
L/V1	22 (12.5)
NA	138 (78.4)
Pn	
Pn0	11 (6.3)
Pn1	12 (6.8)
NA	151 (85.8)

*Detailed clinical data and histopathological information were available for 174 patients.
[†]Overall survival was available for n = 160 patients.
[‡]Twelve patients with resection and 2 patients with biopsy at the time of diagnosis received liver transplantation afterward.
[§]Cases with NA for pN had no lymph nodes resected; therefore, AJCC status could not be assessed.
[‖]NOS = typical ductal/glandular/tubular/acinar histologic phenotype of BTC.
Abbreviations: G, grade of differentiation; L/V, invasion into lymphatic vessels/veins; M, distant metastases; NA, not available; pN, histopathologic lymph node evaluation; Pn, perineural invasion; pT, histopathologic tumor stage evaluation; R, resection margins.

stimulating activity polypeptide 1], and *TGFBR2*) in the BTC subgroups iCCA, pCCA, dCCA, and GBC (Supporting Table S8).[(15)]

We examined associations between genomic alterations and overall survival using the endpoint of BTC-related death. Only one patient died due to a PSC-unrelated cause and was therefore censored. The baseline time point used in the survival analysis was BTC diagnosis. Statistical analysis and visualization was performed using the computing environment R (http://www.R-project.org/) and GraphPad Prism 6. Median survival and the corresponding 95% confidence intervals were calculated by Kaplan-Meier survival analysis, and the survival distributions for each category were compared using the log-rank test. All reported *P* values were two-sided, and *P* < 0.05 was
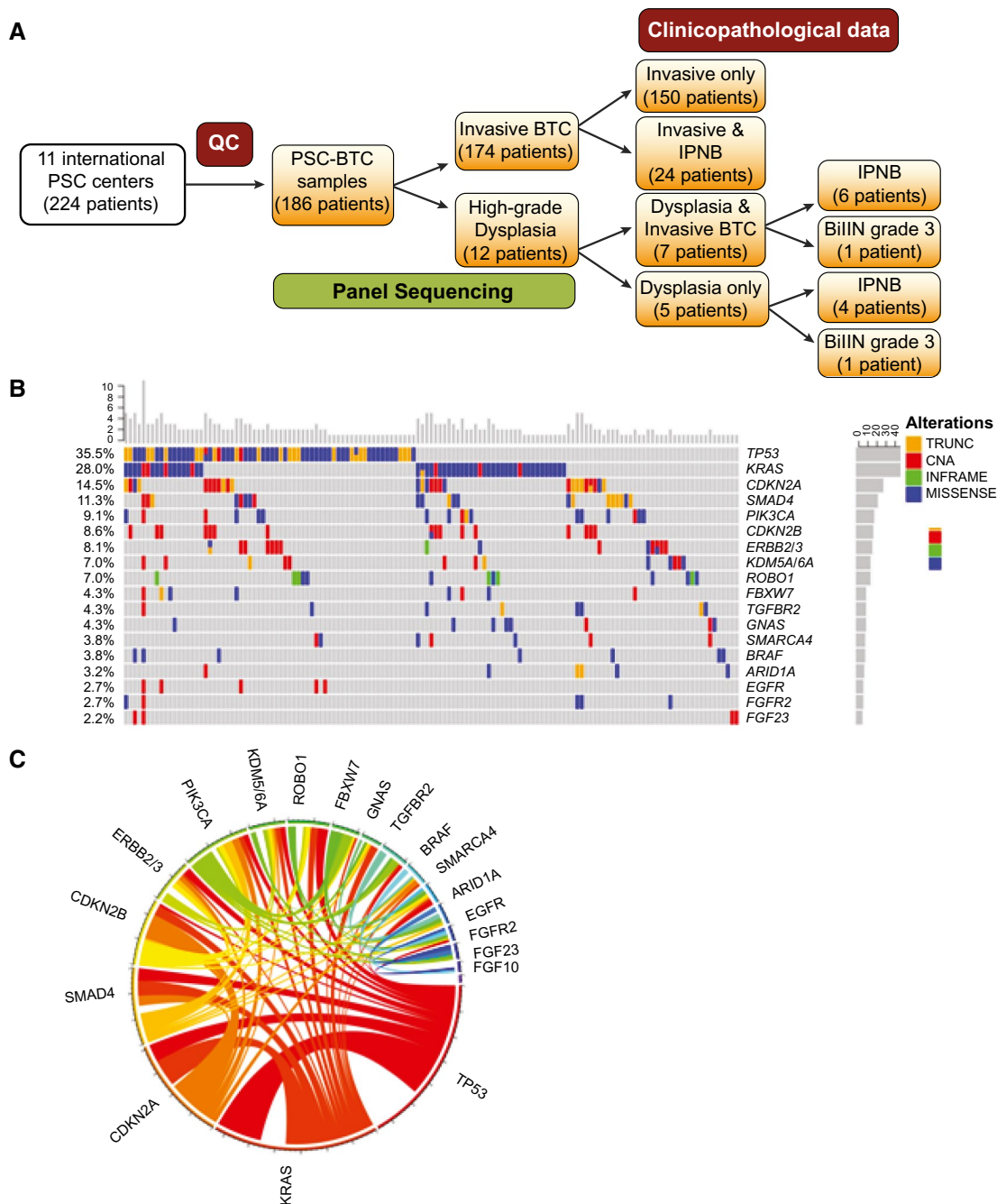
FIG. 1. Mutational landscape of PSC-BTCs. (A) Schematic overview of the study design. (B) Oncoplots of genes sorted by frequency of mutations in all BTC samples. Missense mutations, inframe mutations, truncations, and CNAs with frequencies greater than 2% across the panel of PSC-BTC patients (n = 186). (C) Circos plot representing co-occurrence of mutations. A band connecting genes represents co-occurring mutations in a given patient. The width of the band represents the frequency of this mutation pair within the data set. Abbreviations: CNA, copy number alteration; TRUNC, truncation; QC, quality control.

considered statistically significant. Enrichment analysis was done using Fisher's exact test. If more than two groups were compared, pairwise comparisons were done for all combinations using Fisher's exact test, and false-discovery rate correction of the P values was performed according to Benjamini-Hochberg.

Graphical representations of mutational differences by oncoplot and circos plots were created by the
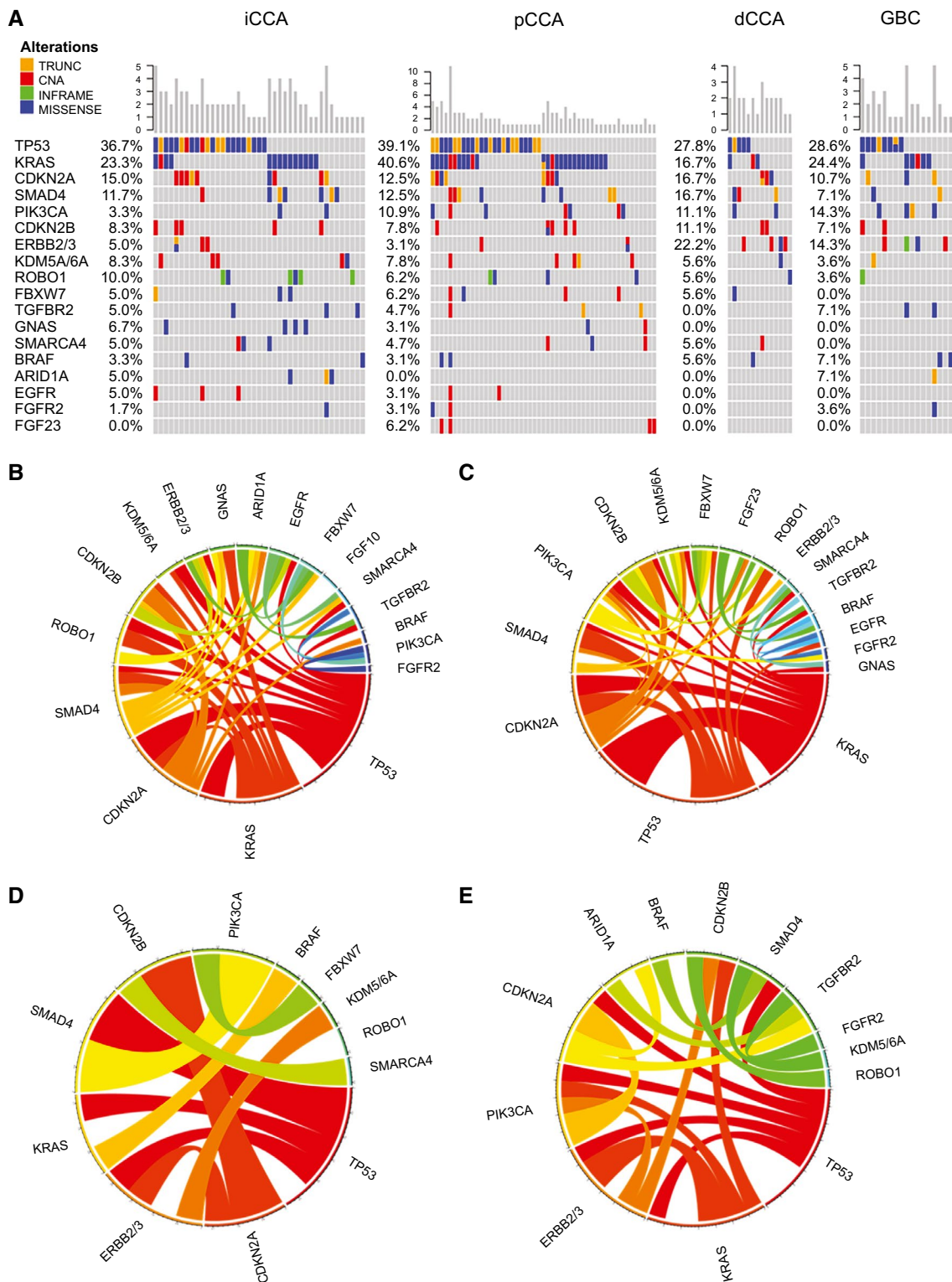
FIG. 2. Mutational landscape of different subtypes of PSC-associated BTC. (A) Oncoplots of genes sorted by frequency of mutations in all BTC subtypes. Missense mutations, inframe mutations, TRUNCs, and CNAs of 146 patients with recurrent mutations are shown. Circos plots depicting interrelationships of mutations stratified by PSC-BTC-subtypes: iCCA (B), pCCA (C), dCCA (D), and GBC (E).

publicly available R-package circlize (see Supporting Information).[16]

Putative actionable targets were identified using the TARGET (tumor alterations relevant for genomics-driven therapy) database version 3 by Broad Institute (http://archive.broadinstitute.org/cancer/cga./target).[17]

Results

CLINICAL CHARACTERISTICS

Tumor samples from 186 patients with PSC-BTC, including 174 (93.5%) invasive carcinomas and 12 (6.5%) high-grade noninvasive biliary neoplasms, were analyzed by panel sequencing (Table 1 and Fig. 1). The panel of patients with PSC-BTC showed a male preponderance (128 of 174; 73.6%; Table 2). The mean age at diagnosis of PSC was 41.6 years (range: 11.9-73.5 years), and at diagnosis of BTC was 48.1 years. Overall survival of patients with PSC- was poor, with a 5-years survival rate of 21.6% (n = 160; Table 2).

HISTOMORPHOLOGY AND PANEL SEQUENCING REVEALED AN EXTRAHEPATIC PHENOTYPE OF PSC-BTC

According to the anatomical location, the patient panel consisted of 60 iCCAs, 64 pCCAs, 18 dCCAs, 28 GBCs, and 4 samples of unknown anatomical origin (Table 1). CCA was sampled from explant liver tissue obtained at liver transplantation in 37 of 186 patients (9 iCCAs, 24 pCCAs, 2 dCCAs, and 2 with unknown anatomical origin). Among the 37 patients with findings of CCA in explant liver, 30 of 37 (81.1%) were incidental findings, whereas 7 of 37 (18.9%) among the CCAs were diagnosed before the transplant.

Analysis of available clinicopathological data and histomorphological evaluation revealed a relatively high frequency of non-NOS histologic subtypes. In detail, only 74 of 174 (44.8%) of the invasive PSC-BTCs showed a typical NOS (ductal/glandular/tubular/acinar) histomorphology, whereas 96 of 174 (55.2%) showed a non-NOS histomorphology (i.e., papillary, mucinous, solid, diffuse, intestinal, or adenosquamous) (Table 2). A cholangiolar/small-duct

histology was observed in only one (1 of 60, 1.7%) iCCA. Moreover, 34 patients with PSC-BTCs (18.3%) showed intraductal or intracystic papillary neoplasms of the bile duct (PSC-IPNB). Of these 34 patients with PSC-IPNB, 30 were associated with invasive CCA, whereas 4 patients had IPNB without invasive CCA (Fig. 1A). Two patients with high-grade precursor biliary intraepithelial neoplasm with grade 3 (BilIN-3) lesions were included: one BilIN-3 was associated with invasive BTC and one was not (Fig. 1A and Supporting Fig. S1). Tumor grading was performed for the invasive carcinomas and showed a predominance of moderate grade (131 of 174; 74.4%) (Table 2).

In 146 (78.5%) of the 186 BTC samples analyzed by massive parallel sequencing, a total of 247 nonsynonymous mutations and 89 copy number alterations (CNAs) in 30 of 42 targeted genes were identified (Fig. 1B and Supporting Table S6). Principal component analysis (PCA) of the mutational profiles revealed that patient samples did not cluster by clinical center or by AJCC staging (Supporting Fig. S2B). Among the 247 nonsynonymous mutations identified, 184 mutations were missense mutations, 56 were truncations, and 7 were in-frame insertions or deletions (Supporting Tables S6 and S7). Genomic alterations within *TP53* (35.5%, including 34.4% missense mutations and truncations), *KRAS* (28.0%, including 24.7% missense mutations), *CDKN2A* (14.5%, including 7% deletions), *SMAD4* (11.4%), *PIK3CA* (9.1%), *CDKN2B* (8.6%), *ERBB2* (8.1%), *KDM5A/6A* (7.0%), and *ROBO1* (7.0%) were most common, with a second tier of less frequently mutated genes (2%-5%) including *FBXW7*, *TGFBR2*, *GNAS*, *SMARCA4* (SWI/SNF Related, Matrix Associated, Actin Dependent Regulator Of Chromatin, Subfamily A, Member 4), *BRAF*, and *ARID1A* (AT-Rich Interaction Domain 1A) (Fig. 1B). Interrelationships among the genes harboring nonsynonymous mutations showed that co-occurrences of *TP53* with *KRAS* alterations and *KRAS* with *CDKN2A* were most common (Fig. 1C). Transitions of both C to T and G to A mutations (C > T | G > A) represented the predominant mutation in all subtypes. The number of mutations per tumor ranged from one to six with a mean of 1.84 ± 1.12 (mean ± SD) mutations per tumor. The mean number of nonsynonymous mutations per tumor was 2.06 ± 1.39 for GBC, 1.86 ± 1.10 for CCA, and 1.36 ± 0.50 for the noninvasive high-grade dysplastic precursor lesions (HGDs). Thus, CCA and GBC shared a comparable number of mutations per sample, whereas

the mean number of mutations in HGDs was significantly lower compared with the invasive BTC samples (P = 0.01). CNAs were found primarily in *CDKN2B* (7.5%), *CDKN2A* (7.0%), and *ERBB2* (4.3%).

In 40 tumors (21.5%), no mutation was detected by panel sequencing of the 42 targeted genes. In the entire patient panel, including n = 60 iCCAs, no *FGFR* translocation or deleterious *BRCA1/2* mutation and only one *IDH1* (p.R132C) mutation (in a single CCA with typical small-duct/cholangiolar histomorphology) were detected (Fig. 2A and Supporting Table S6).[18]

PUTATIVE ACTIONABLE TARGETS IN PSC-BTC

Of the 30 genomically altered genes, 19 are considered actionable according to the TARGET database version 3 by the Broad Institute.[17] A total of 116 (62.4%) samples had mutations within one or more potentially actionable genes, and 49 samples (26.3%) had two or more potentially actionable genes (see Supporting Table S9 for full results).

For a subset of the PSC-BTC panel (n = 95), we were able to construct a TMA and perform additional analyses using IHC and CISH (Supporting Fig. S3). Using the guidelines for HER2 testing in gastric cancer, 8 of 95 (8.4%) cases showed HER2 amplification (see Supporting Table S3). Additionally, immunoreactivity was observed in 39 of 82 (47.6%) patients for epidermal growth factor receptor (EGFR), in 29 of 87 (33.3%) for c-Met, in 1 of 88 (1.1%) for c-Myc, and in 20 of 84 (23.8%) of the analyzed PSC-BTCs for programmed death ligand 1 (PD-L1). MSI analysis using mononucleotide MSI markers (BAT25, BAT26, and CAT25) and IHC for the DNA mismatch repair proteins (MSH2, MSH6, MLH1, and PMS2) revealed no MSI-high case in all analyzed PSC-BTCs (0 of 95). Detailed results of IHC analyses are found in Supporting Table S3.

CORRELATION OF MOLECULAR ALTERATIONS WITH CLINICOPATHOLOGICAL DATA AND FOLLOW-UP

Comparison of the three anatomical subgroups of PSC-associated BTC, including CCA (iCCA, pCCA, and dCCA) and GBC, showed a homogenous mutation profile with no statistically significant differences in frequencies of detected genomic alterations (Fisher's exact test; Fig. 2A and Supporting Figure S4). The interrelationship analysis by circos plots performed in all BTC subtypes separately showed a similar picture (Fig. 2B-E).

Clinical follow-up data were available for 160 of the 186 PSC-BTC patients. During follow-up, as many as 60% of the patients received liver transplantation, which was associated with significantly prolonged patient survival (Supporting Fig. S5 and Table S4). Patient overall survival showed stratification by tumor AJCC stages (P < 0.001; Fig. 3A). Correlation analyses between the mutational profiles did not show statistically significant associations with histological phenotype and AJCC staging (Fisher's exact test). In addition, comparison of the number of nonsynonymous mutations in PSC-BTC subtype-specific analyses was not statistically significant (Fisher's exact test). No statistically significant association between the number of detected molecular alterations in PSC-BTCs and patient overall survival was found (Supporting Fig. S6). Observed center-specific differences in patient overall survival were correlated with differences of tumor AJCC stages between the contributing centers. Patient subtypes and clinicopathological data are described in detail in Table 2 for the entire patient panel and in Supporting Table S1 stratified by contributing centers.

The histomorphological phenotype was associated with overall survival in patients with PSC-BTC. A solid growth pattern showed a significantly shortened overall survival compared with all other histological phenotypes, whereas papillary histology showed a better overall survival compared with other histomorphological subtypes (Fig. 3B).

The analysis of single mutations with overall patient survival revealed significant negative effects on overall survival in patients with tumors harboring mutations in *KRAS* (n = 46, P = 0.027; Fig. 4A-D and Supporting Fig. S7). Patients with nonsynonymous mutations in more than one of the analyzed genes did not show statistically significant differences in overall survival (Supporting Fig. S6).

Discussion

We present herein an integrated morphological and genomic analysis of a large and clinicopathologically
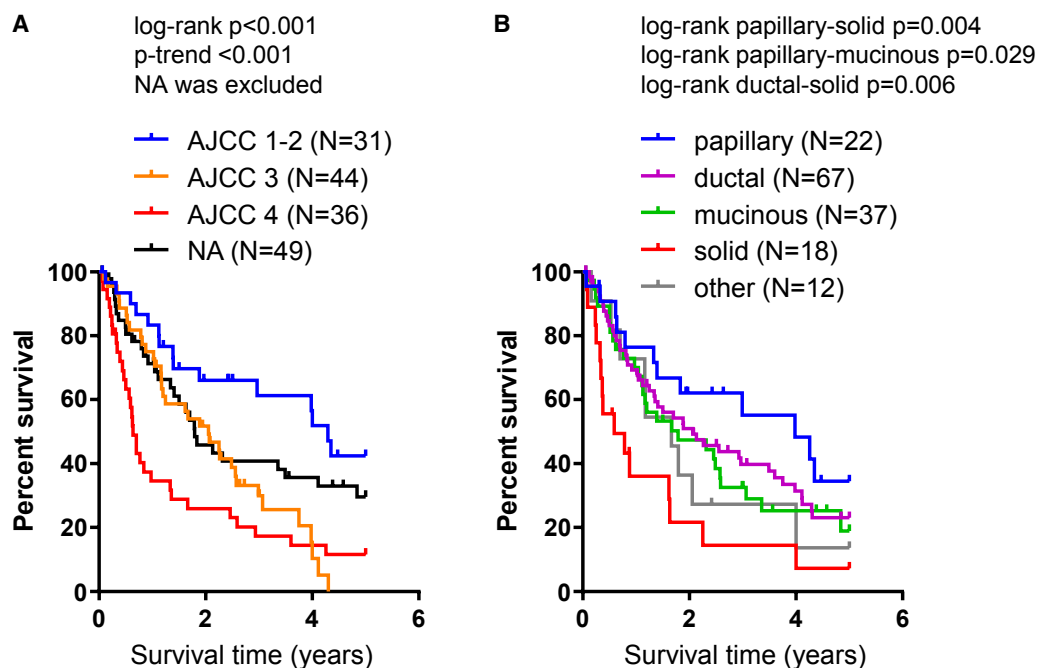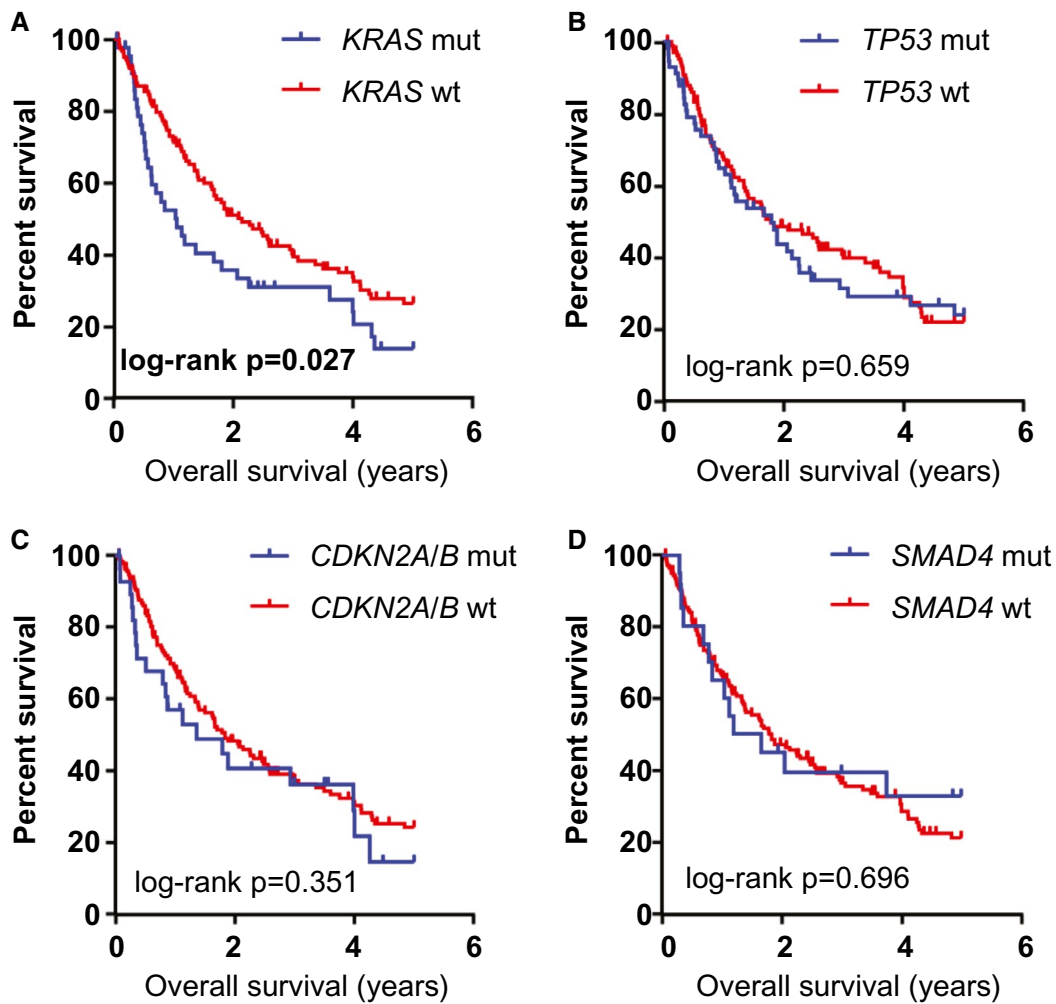
FIG. 3. Overall survival data of patients with PSC-BTC. (A) Overall survival data of 160 of the 186 analyzed patients with PSC-BTC stratified by AJCC staging. (B) Overall survival data of all analyzed patients with PSC-BTC stratified by histological phenotype. Abbreviations: AJCC, American Joint Committee on Cancer Classification; NA, not available.

well-characterized PSC-BTC patient panel. Despite limitations posed by the FFPE basis, which restricted the assessment to targeted resequencing while allowing statistical power through sample size, our data define a common histomorphologic phenotype and the predominant molecular alterations in PSC-driven biliary carcinogenesis. Importantly, we identified a number of potential targets for individualized therapy in a patient group that is currently largely devoid of nonsurgical management options.

Previous studies have documented that genomic alterations in BTC differ according to etiology and anatomical location.[11-15] With regard to etiology, our BTC panel is exceptionally homogenous, as all BTC samples in the cohort were derived from a monoetiological background of PSC. The analysis of a large number of samples from a single BTC etiology allowed us to correlate the molecular findings with various clinicopathological data and anatomical location for common motifs of PSC-BTC. Genomic differences among the anatomical subtypes have been driven primarily by mutations in certain genes, but also partly by variability in gene sets mutated across subtypes.[11,15] A key finding of our study is that

PSC-BTC exhibits a phenotype that is characteristic of extrahepatic, large-duct BTC, independent of the anatomical location of the tumor.[11-14] When comparing the mutational frequencies of the most commonly mutated genes in our PSC-BTC panel with the data published on polyetiological, mostly non-PSC-associated BTCs, we observed that our PSC-BTC panel showed mutational frequencies that are well comparable to extrahepatic CCAs (including pCCA and dCCA).[15] Importantly, this observation includes a large number of tumors with an intrahepatic location (34.5% of the panel), which were still histologically and molecularly indistinguishable from PSC-CCAs of extrahepatic origin. Furthermore, these intrahepatic tumors lacked the genomic alterations characteristic of iCCA (e.g., *IDH1/2* mutations and *FGFR2* translocations).[11,18]

Among the 60 intrahepatic tumors in our panel, signature mutations of iCCA were absent, except for a single case with an *IDH1*-mutation that also included the only case in the patient panel with a small duct/cholangiolocellular histomorphology otherwise present in up to 40% of iCCAs.[18,20] This mutation may have occurred sporadically in this patient. Noteworthy,

FIG. 4. Overall survival data of patients with PSC-BTC in correlation to specific molecular alterations: *KRAS* (A), *TP53* (B), *CDKN2A/B* (C), and *SMAD4* (D). Abbreviations: MT, mutated; WT, wild type.

FGFR2 translocations, otherwise frequently observed in iCCA, were completely absent from the entire PSC-BTC patient panel, including all intrahepatic tumors.[11,14] Likewise, the histomorphological phenotype of our PSC-BTC cohort showed two main differences from non-PSC-BTC: (1) The small-duct type iCCA, now recognized as a distinct subtype of iCCA, was virtually not present in our monoetiological PSC-BTC cohort (1 of 60, 1.7%), and (2) all other PSC-iCCA showed the large-duct type (59 of 60, 98.3%), which is equivalent to an extrahepatic histomorphological phenotype, as seen in pCCA. In the non-PSC-BTC cohort, rarely seen non-NOS (i.e., non-ductal/glandular/tubular/acinar) histologic patterns were very frequent in our PSC-BTC cohort (i.e.,

96 of 174 [55.2%] showed a non-NOS histomorphology [e.g., papillary, mucinous, solid, diffuse, intestinal, or adenosquamous]).

Taken together, PSC-BTC displays a predominantly large-duct BTC genotype and phenotype that presumptively result from common carcinogenic pathways. This is of relevance for molecular testing and for planning of clinical trials of targeted therapies.[18,20]

The mutational profile of PSC-BTC is similar to that observed in liver fluke–related BTC. Corresponding to the genomic profile in our PSC-BTC panel, fluke-positive CCAs are enriched in *TP53, SMAD4, ERBB2,* and *GNAS* alterations, while fluke negative CCAs frequently exhibit *IDH1/2* and

FGFR-related alterations.[12-14] One explanation may be that both PSC and liver fluke disease represent chronic inflammatory conditions, which together with disruption of host bile homeostasis, result in chronic damage of bile duct epithelia and oxidative stress, predisposing to comparable oncogenic mutations. Another explanation may be the common cellular origin, as both conditions primarily affect large intrahepatic and extrahepatic bile ducts.[20,21] Differences between our PSC-BTC panel and available data from both sporadic-related and fluke-related BTC exist regarding the higher frequency of *HER2* (*ERBB2*) alterations, identified in our panel predominantly in dCCAs (22.2%; 4 of 18) and GBC (14.3%; 4 of 28), but present in all anatomical subgroups.[11-15]

Unlike the situation in many other cancers, no targeted treatment options are yet approved for BTC. The scarcity of therapeutic options, together with the lack of sensitive screening options, leads to high mortality and poses an important unmet clinical need in patients with PSC. Thus, to identify genomic alterations amenable to drugs approved for other tumor types or currently tested in clinical trials is of major interest. We detected potentially actionable mutations in 116 (62.4%) of the included patients according to the TARGET database (Supporting Table S8).[17] Examples include alterations in genes affecting PI3K/Akt/mammalian target of rapamycin (e.g., *PIK3CA*, *FBXW7*), RAS/RAF/MEK/ERK (*KRAS*, *BRAF*, *NRAS*), and tyrosine kinase receptor signaling (e.g., *EGFR* [*ERBB1*], *HER2* [*ERBB2*], *ERBB3*, *FGFR2*). *ERBB2* mutations were identified in 8.1% (15 of 186) of the PSC-BTCs in our panel, and 8.4% (8 of 95) of the IHC/CISH accessible cases showed HER2 amplifications. Anti-HER-2 treatment is approved long-term for breast cancer, stomach cancer, and gastroesophageal junction cancer with HER-2 overexpression/amplification.[22-24] Several anti-HER2 clinical trials and case reports show that HER2 is a promising target in BTC, but anti-HER2 agents are still not approved for routine administration in BTC.[25] *EGFR* alterations were identified in 2.7% (5 of 186) of our cases. The anti-EGFR antibody cetuximab is approved for treatment of metastatic colorectal cancer with wild-type K and N-RAS genes.[26] Various EGFR antibodies (cetuximab, erlotinib, and panitumumab) have been analyzed in various combinations with gemcitabine in advanced BTC in phase 2 and 3 clinical studies, but the clinical benefit of EGFR inhibitors in BTC is still unclear, and biomarkers predicting potential response to EGFR inhibition are needed.[27] Other targets with future treatment potential include CDKN2A/2B, which can be targeted by CDK4/6 inhibitors such as palbociclib, which have been applied for the treatment of breast cancer and currently are tested in phase 3 trials in pancreatic cancer (NCT03065062).[28]

Although we failed to detect MSI-high tumors in our PSC-BTC panel, immunoreactivity for PD-L1 was observed in 23.8% (20 of 84) of our cases, suggesting a therapeutic potential of immune checkpoint inhibitors.[29] Immunoreactivity for c-Met was observed in 33.3% (29 of 87) cases, indicating a potential for Met-targeted agents in PSC-BTC. Based on our data, further preclinical research and clinical studies are now warranted to explore the role of the molecular targets observed in PSC-BTC.

Prior genomic analyses in PSC-BTC have been limited to sequencing of *KRAS* and *CDKN2A* genes performed in considerably smaller PSC-BTC panels (n = 10-33 patients).[30-33] We found *KRAS* mutations in 28% of PSC-BTC, a number that is in line with previous studies.[30,31] Supported by our results, previous studies have also implicated *CDKN2A* inactivation in PSC-BTC carcinogenesis.[33] Presence of *TP53* mutations in PSC-BTC have previously only been investigated indirectly by estimating the accumulation of the *TP53*-encoded p53 protein in tumor tissue by IHC.[30-32] Reported rates of p53 overexpression show large variability in previous studies (31%-79%), which may be attributed to the detection mode of altered p53 expression as well as patient selection bias.[30-32] The current *TP53* mutation frequency of 35.5% in PSC-BTC is likely a robust estimate, given the size and broad representation of the current patient panel.

Histomorphological evaluation of the PSC-BTC panel showed a high prevalence of rare histologic phenotypes.[34] Most prominently, a papillary subtype was frequent in PSC-BTC of all anatomical subtypes. This is in line with the finding that IPNB lesions were also more frequent in comparison to previous reports on non-PSC-associated BTC.[35] These morphological findings may reflect the different environmental and molecular setting of PSC versus non-PSC-associated biliary carcinogenesis. Future mechanistic studies should attempt to elaborate on IPNB as a precursor lesion of PSC-BTC.

Obvious limitations of this study are the retrospective character of the tissue and data collection as well as the limited genomic coverage intrinsic to the panel-sequencing approach. To enable a statistically informative study in this rare group of BTC, in which prospectively collected fresh frozen tissue is extremely scarce, we focused our recruitment on establishing an adequately sized archived FFPE PSC-BTC material from explant livers, surgical resections, or biopsies. The panel sequencing approach allowed for the use of FFPE material from these sources with an acceptable rate of excluded samples (17%; 38 of 224 samples) due to insufficient tumor material or low DNA content or quality. Selection bias, and putatively also a center bias, may have been introduced by indirectly enriching for resected and transplanted cases (i.e., an overrepresentation of lower-stage cases). Despite this limitation, a distribution of patients across all four AJCC stages was still achieved. Retrospective data also led to some degree of missing data, and together with the high transplantation frequency, limits the validity of survival analyses for certain subtypes, including the assessment of putatively prognostic mutations. Despite limitations, the study represents a major advance in being the largest molecular characterization of PSC-BTC to date, and the analysis of histopathological, clinical, and follow-up data allowed for several significant conclusions to be drawn.

In conclusion, our study demonstrated a common morpho-molecular phenotype across all anatomical locations of PSC-BTC. We also detected several genetic abnormities relevant for future research into potential targeted therapies in this underserved patient group. Further characterization of PSC-BTC tissue panels and single cells using whole-exome and whole-genome sequencing in future studies is likely to expand on current observations.

REFERENCES

1) Weismuller TJ, Trivedi PJ, Bergquist A, Imam M, Lenzen H, Ponsioen CY, et al. Patient age, sex, and inflammatory bowel disease phenotype associate with course of primary sclerosing cholangitis. Gastroenterology 2017;152:1975-1984.e8.

2) Boonstra K, Weersma RK, van Erpecum KJ, Rauws EA, Spanier BW, Poen AC, et al. Population-based epidemiology, malignancy risk, and outcome of primary sclerosing cholangitis. HEPATOLOGY 2013;58:2045-2055.

3) Bergquist A, Ekbom A, Olsson R, Kornfeldt D, Loof L, Danielsson A, et al. Hepatic and extrahepatic malignancies in primary sclerosing cholangitis. J Hepatol 2002;36:321-327.

4) Tanaka A, Takamori Y, Toda G, Ohnishi S, Takikawa H. Outcome and prognostic factors of 391 Japanese patients with primary sclerosing cholangitis. Liver Int 2008;28:983-989.

5) Choi J, Ghoz HM, Peeraphatdit T, Baichoo E, Addissie BD, Harmsen WS, et al. Aspirin use and the risk of cholangiocarcinoma. HEPATOLOGY 2016;64:785-796.

6) Jusakul A, Kongpetch S, Teh BT. Genetics of Opisthorchis viverrini-related cholangiocarcinoma. Curr Opin Gastroenterol 2015;31:258-263.

7) **Ali AH**, **Tabibian JH**, Nasser-Ghodsi N, Lennon RJ, DeLeon T, Borad MJ, et al. Surveillance for hepatobiliary cancers in patients with primary sclerosing cholangitis. HEPATOLOGY 2018;67:2338-2351.

8) Chapman R, Fevery J, Kalloo A, Nagorney DM, Boberg KM, Shneider B, et al. Diagnosis and management of primary sclerosing cholangitis. HEPATOLOGY 2010;51:660-678.

9) Rosen CB, Heimbach JK, Gores GJ. Liver transplantation for cholangiocarcinoma. Transpl Int 2010;23:692-697.

10) Valle J, Wasan H, Palmer DH, Cunningham D, Anthoney A, Maraveyas A, et al. Cisplatin plus gemcitabine versus gemcitabine for biliary tract cancer. N Engl J Med 2010;362: 1273-1281.

11) **Nakamura H**, **Arai Y**, **Totoki Y**, **Shirota T**, **Elzawahry A**, Kato M, et al. Genomic spectra of biliary tract cancer. Nat Genet 2015;47:1003-1010.

12) **Ong CK**, **Subimerb C**, Pairojkul C, Wongkham S, Cutcutache I, Yu W, et al. Exome sequencing of liver fluke-associated cholangiocarcinoma. Nat Genet 2012;44:690-693.

13) **Chan-On W**, **Nairismagi ML**, **Ong CK**, **Lim WK**, Dima S, Pairojkul C, et al. Exome sequencing identifies distinct mutational patterns in liver fluke-related and non-infection-related bile duct cancers. Nat Genet 2013;45:1474-1478.

14) **Jusakul A**, **Cutcutache I**, **Yong CH**, **Lim JQ**, Huang MN, Padmanabhan N, et al. Whole-genome and epigenomic landscapes of etiologically distinct subtypes of cholangiocarcinoma. Cancer Discov 2017;7:1116-1135.

15) **Wardell CP**, **Fujita M**, Yamada T, Simbolo M, Fassan M, Karlic R, et al. Genomic characterization of biliary tract cancers identifies driver genes and predisposing mutations. J Hepatol 2018;68:959-969.

16) Gu Z, Eils R, Schlesner M. Complex heatmaps reveal patterns and correlations in multidimensional genomic data. Bioinformatics 2016;32:2847-2849.

17) **Van Allen EM**, **Wagle N**, Stojanov P, Perrin DL, Cibulskis K, Marlow S, et al. Whole-exome sequencing and clinical interpretation of formalin-fixed, paraffin-embedded tumor samples to guide precision cancer medicine. Nat Med 2014;20:682-688.

18) Liau JY, Tsai JH, Yuan RH, Chang CN, Lee HJ, Jeng YM. Morphological subclassification of intrahepatic cholangiocarcinoma: etiological, clinicopathological, and molecular features. Mod Pathol 2014;27:1163-1173.

19) Goeppert B, Toth R, Singer S, Albrecht T, Lipka DB, Lutsik P, Brocks D, et al. Integrative analysis defines distinct prognostic subgroups of intrahepatic cholangiocarcinoma. J Hepatol 2019;69:2091-2106.

20) Brandi G, Farioli A, Astolfi A, Biasco G, Tavolari S. Genetic heterogeneity in cholangiocarcinoma: a major challenge for targeted therapies. Oncotarget 2015;6:14744-14753.

21) Carpino G, Cardinale V, Folseraas T, Overi D, Grzyb K, Costantini D, et al. Neoplastic transformation of peribiliary stem cell niche in cholangiocarcinoma arisen in primary sclerosing cholangitis. Hepatology 2019;69:622-638.

22) Ross JS, Slodkowska EA, Symmans WF, Pusztai L, Ravdin PM, Hortobagyi GN. The HER-2 receptor and breast cancer: ten years of targeted anti-HER-2 therapy and personalized medicine. Oncologist 2009;14:320-368.

23) **Bang YJ**, **Van Cutsem E**, Feyereislova A, Chung HC, Shen L, Sawaki A, et al. Trastuzumab in combination with chemotherapy versus chemotherapy alone for treatment of HER2-positive advanced gastric or gastro-oesophageal junction cancer (ToGA): a phase 3, open-label, randomised controlled trial. Lancet 2010;376:687-697.

24) Muller V, Clemens M, Jassem J, Al-Sakaff N, Auclair P, Nuesch E, et al. Long-term trastuzumab (Herceptin) treatment in a continuation study of patients with HER2-positive breast cancer or HER2-positive gastric cancer. BMC Cancer 2018;18:295.

25) Yarlagadda B, Kamatham V, Ritter A, Shahjehan F, Kasi PM. Trastuzumab and pertuzumab in circulating tumor DNA ERBB2-amplified HER2-positive refractory cholangiocarcinoma. NPJ Precis Oncol 2019;3:19.

26) Cunningham D, Humblet Y, Siena S, Khayat D, Bleiberg H, Santoro A, et al. Cetuximab monotherapy and cetuximab plus irinotecan in irinotecan-refractory metastatic colorectal cancer. N Engl J Med 2004;351:337-345.

27) Tariq NU, McNamara MG, Valle JW. Biliary tract cancers: current knowledge, clinical candidates and future challenges. Cancer Manag Res 2019;11:2623-2642.

28) Beaver JA, Amiri-Kordestani L, Charlab R, Chen W, Palmby T, Tilley A, et al. FDA approval: palbociclib for the treatment of postmenopausal patients with estrogen receptor-positive, HER2-negative metastatic breast cancer. Clin Cancer Res 2015;21:4760-4766.

29) Lote H, Cafferkey C, Chau I. PD-1 and PD-L1 blockade in gastrointestinal malignancies. Cancer Treat Rev 2015;41:893-903.

30) Boberg KM, Schrumpf E, Bergquist A, Broome U, Pares A, Remotti H, et al. Cholangiocarcinoma in primary sclerosing cholangitis: K-ras mutations and Tp53 dysfunction are implicated in the neoplastic development. J Hepatol 2000;32:374-380.

31) Ahrendt SA, Rashid A, Chow JT, Eisenberger CF, Pitt HA, Sidransky D. p53 overexpression and K-ras gene mutations in primary sclerosing cholangitis-associated biliary tract cancer. J Hepatobiliary Pancreat Surg 2000;7:426-431.

32) Rizzi PM, Ryder SD, Portmann B, Ramage JK, Naoumov NV, Williams R. p53 Protein overexpression in cholangiocarcinoma arising in primary sclerosing cholangitis. Gut 1996;38: 265-268.

33) Taniai M, Higuchi H, Burgart LJ, Gores GJ. p16INK4a promoter mutations are frequent in primary sclerosing cholangitis (PSC) and PSC-associated cholangiocarcinoma. Gastroenterology 2002;123:1090-1098.

34) Goeppert B, Frauenschuh L, Zucknick M, Stenzinger A, Andrulis M, Klauschen F, et al. Prognostic impact of tumour-infiltrating immune cells on biliary tract cancer. Br J Cancer 2013;109:2665-2674.

35) Schlitter AM, Born D, Bettstetter M, Specht K, Kim-Fuchs C, Riener MO, et al. Intraductal papillary neoplasms of the bile duct: stepwise progression to carcinoma involves common molecular pathways. Mod Pathol 2014;27:73-86.

Author names in bold designate shared co-first authorship.

Supporting Information

Additional Supporting Information may be found at onlinelibrary.wiley.com/doi/10.1002/hep.31110/suppinfo.